



Colorimetric detection of cephadrine in pharmaceutical formulations via fluorosurfactant-capped gold nanoparticles

Chao Lu*, Nan Zhang, Jinge Li, Qianqian Li

State Key Laboratory of Chemical Resource Engineering, Beijing University of Chemical Technology, Beijing 100029, China

ARTICLE INFO

Article history:

Received 8 November 2009

Received in revised form 3 January 2010

Accepted 4 January 2010

Available online 11 January 2010

Keywords:

Cephadrine

Gold nanoparticles

Fluorosurfactant

Colorimetric detection

ABSTRACT

The aggregation of gold nanoparticles (GNPs) capped with nonionic fluorosurfactant (FSN) could be induced rapidly and selectively by cephadrine degradation products, but not by cephadrine and other excipients in pharmaceutical formulations. A new detection method for cephadrine has been developed based on the cephadrine degradation products-induced aggregation of the GNPs. The present approach offers various advantages, such as simplicity and high selectivity. Under optimum conditions, the lowest detectable concentration of cephadrine through this approach ($S/N=3$) is $0.8 \mu\text{g mL}^{-1}$. The calibration curve was linear over the range of $2.0\text{--}10.0 \mu\text{g mL}^{-1}$ for the detection of cephadrine. The recoveries of cephadrine were found to fall in the range between 97% and 105%. We have validated the applicability of our method through the analyses of cephadrine in pharmaceutical formulations. Good agreements were obtained for the determination of cephadrine between the present approach and official method.

© 2010 Elsevier B.V. All rights reserved.

1. Introduction

Cephadrine ($\text{C}_{16}\text{H}_{19}\text{N}_3\text{O}_4\text{S}$), a member of the first generation cephalosporins, is widely used in the treatment of bacterial infections of the urinary and respiratory tract, ear, skin and soft tissues, due to its activity against Gram-positive and Gram-negative microorganisms, and its inhibition of bacterial cell wall synthesis [1,2]. Several analytical methods have been developed for cephadrine determination in pharmaceutical formulations including spectrophotometry [3,4], electrochemical technique [5], fluorometry [6,7], and chemiluminescence [8,9]. However, the reported detection methods for cephadrine often suffer from different disadvantages, such as the sophisticated procedures, expensive instrumentation and unsuited analysis for lower concentration range.

Interest is rapidly emerging in the exploration of GNPs for the detection of biological molecules because of their strongly distance-dependent optical properties and large surface areas. Excellent examples included the colorimetric sensing of duplex DNA formation [10–12], protein–ligand interaction [13–15], and metal ion ligand complexation [16–19]. Some researchers were interested in exploring interfacial reactivities of modified GNPs with biologically relevant thiol-containing amino acids such as cysteine, homocysteine and glutathione, leading to the red-shift of

the surface plasmon resonance (SPR) absorption peak, and then developed colorimetric detection methods [20–22]. Thomas and his coauthors used gold nanorods stabilized with cetyltrimethylammonium bromide (CTAB) to detect thiol-containing amino acids [20]. Chen and Chang described the detection of thiols with Nile red-adsorbed gold nanoparticles [21]. Recently, we found that much more rapid aggregation of fluorosurfactant-capped gold nanoparticles (FSN-capped GNPs) could be induced by cysteine and homocysteine at a high temperature (70°C) and in the presence of high salt [23,24]. The results stimulated us to enlarge the application of FSN-capped GNPs for other biomolecules.

Cephadrine is a kind of compound containing sulfur, and its alkaline or acidic degradation can produce thiols [6,25] (Fig. 1). In our study, we found that the FSN-capped GNPs present high selectivity to thiol-containing compounds. The acidic degradation product of cephadrine can produce thiols, while cephadrine without degradation did not contain thiols (see Fig. 1). Therefore, the aggregation of FSN-capped GNPs could be induced by the acidic degradation product of cephadrine but not by cephadrine directly.

Herein, we synthesized 14-nm GNPs capped with FSN, and examined its interaction with cephadrine and its acidic degradation production. It was found the aggregation of GNPs could be induced by its acidic degradation production, but not by cephadrine and other excipients in pharmaceutical formulations, such as glucose and starch. To demonstrate the usefulness of the present method for the determination of cephadrine, the selectivity, recovery, precision, and linear dynamic range were examined. The results showed that the proposed method was developed for the detection of cephadrine in pharmaceutical formulations, and the results were

* Corresponding author. Tel.: +86 10 64411832; fax: +86 10 64411832.

E-mail addresses: luchao@mail.buct.edu.cn, luchao20022002@yahoo.com.cn (C. Lu).

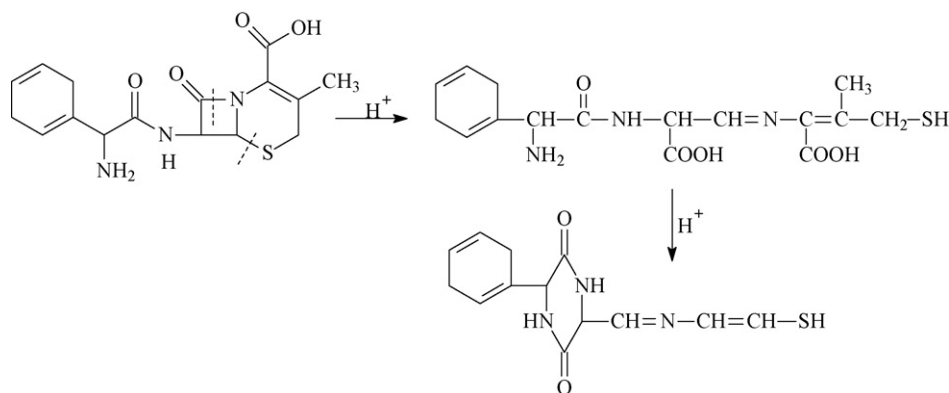


Fig. 1. The process of cephadrine degradation in acidic medium.

compared with certified values. Compared with the other methods for cephadrine, the proposed method showed the wide linear range by tuning the aggregation temperature and higher selectivity (only toward thiols). Although the limit of detection (LOD) is almost same as the reported methods [3–9], it is enough for detection of cephadrine in pharmaceutical formulations.

2. Experimental

2.1. Reagents

All reagents were of analytical grade and used without further purification. Zonyl FSN-100 ($(\text{F}(\text{CF}_2\text{CF}_2)_{1-7}\text{CH}_2\text{O}(\text{CH}_2\text{CH}_2\text{O})_{0-15}\text{H})$) were purchased from Sigma–Aldrich. Hydrogen tetrachloroaurate(III) trihydrate ($\text{HAuCl}_4 \cdot 3\text{H}_2\text{O}$) was purchased from Acros. Cephadrine standard was purchased from National Institute for the Control of Pharmaceutical and Biological Products (Beijing, China). Trisodium citrate and other chemicals were purchased from Beijing Chemical Reagent Company. Cephadrine capsules were supplied by Sino-American Shanghai Squibb Pharmaceuticals Ltd. (Shanghai, China). Cephadrine injections were purchased from Youcare Pharma Ceutical Group Co., Ltd. (Beijing, China). All solutions were prepared with deionized water. The pH of the phosphate buffer solution (PBS) was adjusted with NaOH or HCl. The stock solution of cephadrine (1 mg mL^{-1}) was prepared by dissolving 0.05 g of cephadrine in 50 mL of deionized water. The stock solutions were stored at 4°C until analysis, and working standard solutions were prepared by suitable dilution of the stock solution with deionized water.

2.2. Apparatus

UV–visible spectra were measured on a USB4000 miniature fiber optic spectrometer in absorbance mode with a DH-2000 deuterium and tungsten halogen light source (Ocean Optics, Dunedin, FL) and a HITACHI-800 transmission electron microscope (TEM) (Hitachi High-Technologies Corp., Tokyo, Japan).

2.3. Procedure

2.3.1. Gold nanoparticles synthesis

All glassware used for preparation of GNPs was thoroughly washed with freshly prepared aqua regia ($\text{HNO}_3:\text{HCl} = 1:3$), rinsed extensively with deionized water, and then dried in an oven at 100°C for 2–3 h. Gold nanoparticles of the different sizes were prepared by varying $[\text{Au(III)}]/[\text{citrate}]$ ratio during the reduction step [26]. For example, colloidal GNPs with average diameters of 14 nm were prepared following the literature procedure. Briefly, a 50 mL

solution of 0.04% sodium citrate was brought to a vigorous boil with stirring in a round-bottom flask fitted with a reflux condenser, and then $85 \mu\text{L}$ of 5% HAuCl_4 was added to the stirring and refluxing sodium citrate solution. The solution was maintained at the boiling point with continuous stirring for 15 min. After the solution was allowed to cool to room temperature with continuous stirring, 2 mL of 1% FSN-100 was added. The suspension was stored at 4°C until further use. The TEM specimens were prepared by depositing an appropriate amount of the FSN-capped GNPs onto the carbon-coated copper grids, and excess solution was wicked away by a filter paper. The grid was subsequently dried in air. Assuming spherical particles and density equivalent to that of bulk gold (19.30 g cm^{-3}), the concentration of 14-nm GNPs was calculated to be $\sim 2.9 \text{ nM}$.

2.3.2. Degradation of cephadrine in standard solution and pharmaceutical formulations

Into a series of 10 mL test tube, 0.5 mL of a standard or sample cephadrine solution with different concentrations, 3.25 mL of deionized water, 1.25 mL of 12 M HCl was added. Then, the resulting solution was heated in a boiling-water for about 15 min. After immediately cooled to room temperature in running water, the solution containing degradation products of cephadrine was adjusted to neutral pH with 1.0 M NaOH and then were transferred quantitatively to 10 mL volumetric flask, and the volume was finally completed with deionized water.

3. Results and discussion

3.1. Interaction of FSN-capped GNPs with cephadrine and its degradation products

We examined the spectral changes of the FSN-capped GNP colloids upon the addition of cephadrine and its degradation products. Fig. 2 showed that, upon the addition of $20 \mu\text{g mL}^{-1}$ cephadrine, no spectral change occurred. However, in the presence of $4 \mu\text{g mL}^{-1}$ cephadrine degradation products, the absorption band at 519 nm decreased while new bands appeared at longer wavelengths (600–700 nm), suggesting that FSN ligands allowed thiol–gold interaction while prohibiting the binding of other functional groups on the GNPs. The effects of gold colloids with different sizes on the color change of GNPs induced by cephadrine degradation products were investigated. As shown in Fig. 3, the color change highly depends on the size of gold nanoparticles. The great color change was obtained from 14-nm GNPs, which was chosen as the optimum GNPs size in the further experiments.

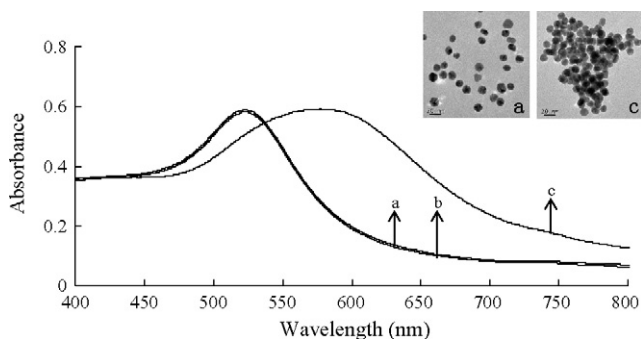


Fig. 2. UV-vis absorption spectra of the 14-nm FSN-capped GNPs (a) in the presence of degradation and undegradation cephradine. The solutions contain $20 \mu\text{g mL}^{-1}$ cephradine (b) and $4 \mu\text{g mL}^{-1}$ cephradine degradation products (c), respectively. All of the solutions contained 90 mM PBS (pH 7.5). The values were acquired at 4 min after addition of the analytes at 60°C . Inset, TEM images of the 14-nm FSN-capped GNPs were in the absence (a) and presence (c) of cephradine degradation products.

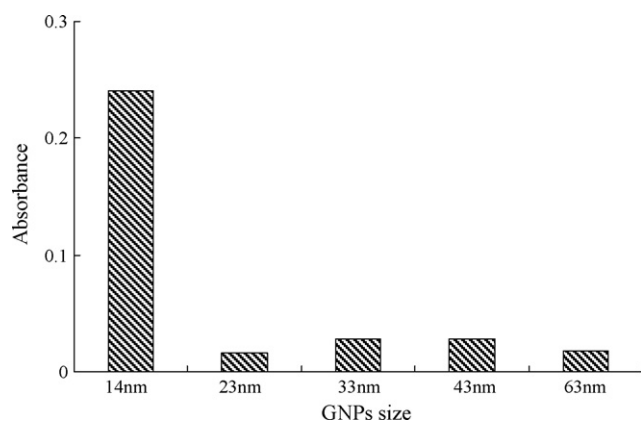


Fig. 3. Effect of GNPs size. The solutions contain $4 \mu\text{g mL}^{-1}$ cephradine degradation products and 90 mM PBS (pH 7.5). The values were acquired at 4 min after addition of the analytes for FSN-capped GNPs at 60°C .

3.2. Optimization of pH and ionic strength of solution

It was found that the solution pH change in the range of 4–10 influenced the rate of the GNPs aggregation obviously. The aggregation rate reached the maximum at pH 7.5. However, the aggregation would slow down when the pH became lower or higher. The aggregation kinetics of FSN-capped GNPs was dependent on the diffusion rate of thiols and the formation of Au–S bonds. When the lower pH for $4 \mu\text{g mL}^{-1}$ cephradine at 60°C was used, HS was dominated due to its protonation. Therefore, it was difficult to make the formation rate of Au–S bonds even at longer time (about 30 min at pH 4). While, in the presence of higher pH, HS was deprotonated to pro-

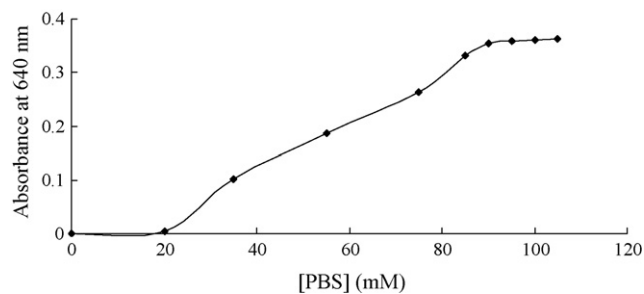


Fig. 4. Salt effect on cephradine degradation products-induced absorbance changes of 14-nm FSN-capped GNPs. The solutions contained $4 \mu\text{g mL}^{-1}$ at pH 7.5. The values were acquired at 4 min after addition of the analytes for 14-nm FSN-capped GNPs at 60°C .

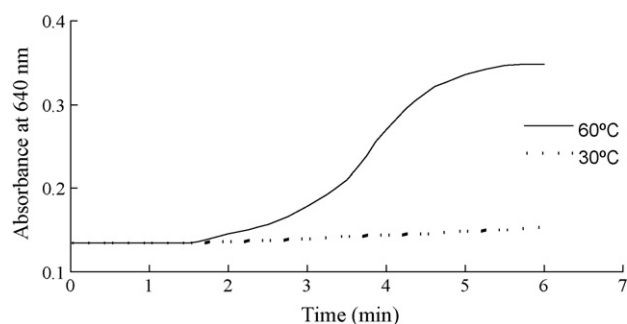


Fig. 5. Time courses of extinction (at 640 nm) of the FSN-capped GNPs upon the addition of $4 \mu\text{g mL}^{-1}$ cephradine degradation products at different temperatures. The solutions contain 90 mM PBS (pH 7.5).

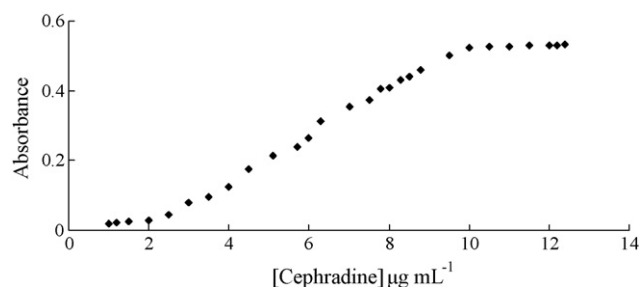


Fig. 6. Absorbance at 640 nm versus cephradine concentration in the standard solution at pH 7.5. The solutions contain 90 mM PBS. The values were acquired at 4 min after addition of the analytes for 14-nm FSN-capped GNPs at 60°C .

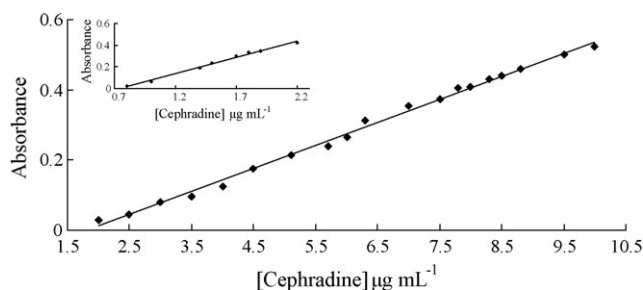


Fig. 7. Calibration curve (absorbance at 640 nm) for detection of cephradine in the standard solution at 60°C . Inset, the calibration curve was obtained at 75°C .

duce S^- , resulting in strong electrostatic repulsion forces between citrate anions and S^- . The GNPs aggregation would slow down (12 min at pH 10) because of its slower diffusion rate. However, when the solution pH was 7.5, both the diffusion rate of thiols and

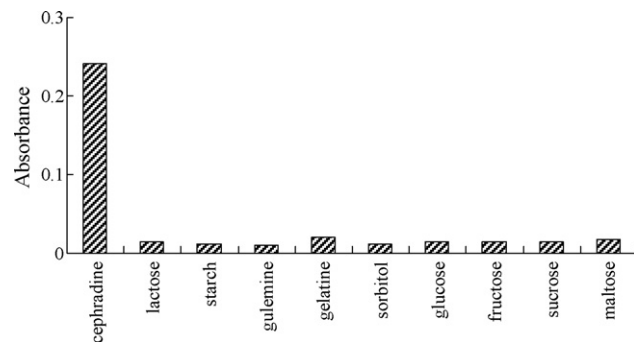


Fig. 8. Absorbance at 640 nm versus some typical interference species in pharmaceutical formulation on the determination of $4.0 \mu\text{g mL}^{-1}$ cephradine degradation products. The solutions contain 90 mM PBS. The values were acquired at 4 min after addition of the analytes for 14-nm FSN-capped GNPs at 60°C .

Table 1
Determination of cephadrine in capsule and injection samples.

Samples	Labeled (g/capsule)	Measured ^a (g)	Added (g)	Found ^a (g)	Recovery (%)
Capsule	0.25	0.245 ± 0.009	0.250	0.245 ± 0.008	98 ± 3.2
			0.100	0.097 ± 0.003	97 ± 3.0
Injection	0.50	0.500 ± 0.019	0.500	0.505 ± 0.013	101 ± 2.6
			0.200	0.204 ± 0.004	102 ± 2.0

^a Mean ± SD of three measurements.

the formation rate of Au–S bonds reached balance, and thus the GNPs aggregation rate was largest (4 min). Therefore, the solution with pH 7.5 was operated throughout this study.

The different buffers, such as PBS, Tris–HCl, sodium citrate–sodium chloride and sodium borate buffer at optimal pH (7.5) are used to investigate toward colorimetric reaction of cephadrine degradation product. The aggregation rate in all kinds of buffer is increased with an increase of ion strength. This is due to the fact that the aggregation could be driven by the London-van der Waals attraction force, which is facilitated under high-salt conditions. When we prepared the different buffers with the same ion strength, the aggregation rate is almost same. In this paper, PBS buffer was chosen as the optimum buffer on account of its higher ion strength in the same buffer concentration as the other buffers.

Fig. 4 showed that the colorimetric evolution of the colloidal solution upon the addition of cephadrine degradation products was affected significantly by PBS (pH 7.5) concentration. The aggregation rate was increased with an increased concentration of PBS from 0 to 90 mM, and then kept at a constant when the concentration of PBS was above 90 mM. This is due to the fact that the aggregation could be driven by the London-van der Waals attraction force, which was facilitated under high-salt conditions. However, the shielding effect of the higher PBS concentrations is saturated for the aggregation GNPs, and thus they were not able to exert further effect on the absorbance signals. In the present study, the optimum concentration of PBS is 90 mM.

3.3. Influence of temperature

It is well-known that the kinetic energy of the particles is increased with the increase of temperature, resulting in higher opportunity and intensity of the mutual collision, which promoted the coalescence of the particles. The influence of temperature on the cephadrine degradation products-induced color change of the GNP colloids in 90 mM PBS was shown in Fig. 5. The aggregation rate of 14-nm FSN-capped GNPs was strongly dependent on the processing temperature. However, the FSN-capped colloidal solution itself displayed aggregation tendency at temperature higher than 80 °C. Moreover, it was noted that there exist a narrow linear range with the increase of temperature from 30 to 80 °C. A temperature of 60 °C was chosen as the optimum condition in view of the detection sensitivity and the linear relationship.

3.4. Analytical performances

Under optimum experimental conditions with 75 °C of the processing temperature, the calibration curve was found to be linear from 0.8 to 2.2 μg mL⁻¹ for cephadrine and the detection limits (S/N = 3) is 0.4 μg mL⁻¹ (see inset in Fig. 7). As shown in Fig. 6, when 75 °C was used for the aggregation of FSN-capped GNPs, the extinction change started to occur when cephadrine concentration was higher than 1.5 μg mL⁻¹. A linear increase was observed in the concentration range of 2.0–10.0 μg mL⁻¹. Further absorbance change was not obvious upon the addition of a larger amount of cephadrine. The standard regression equation between the cephadrine concentration (X) and the absorbance intensity (Y) at 640 nm is

$Y = 0.0656X - 0.119$, and the corresponding regression coefficient is 0.9956 (Fig. 7). The relative standard deviation (RSD) for nine measurements of the 4.0 μg mL⁻¹ cephadrine is 1.8. The limit of detection for cephadrine (S/N = 3) was 0.8 μg mL⁻¹.

3.5. Interferences

To demonstrate the selectivity of the developed method for the detection of cephadrine, the effects of typical interference species in pharmaceutical formulations, such as lactose, starch, gulemine, gelatine, sorbitol, glucose, fructose and sucrose maltose, were investigated. As shown in Fig. 8, the color change of the FSN-capped GNP colloids with and without the presence of these common interference species were almost same, which clearly demonstrated the high selectivity of the present method for the determination of cephadrine. Of course, the other antibiotics, such as cefalexin, cefalotin, cefazoline were also simultaneously detected by this present method after separation.

3.6. Analysis of real samples

In order to evaluate the applicability and reliability of the proposed methodology, it was applied to the determination of cephadrine in commercial pharmaceutical formulations. The analytical merits of the present method were evaluated by comparing the cephadrine contents obtained between the present method and the officially taken method. As shown in Table 1, the results obtained with the two methods were in good agreement for the determination of cephadrine in commercial pharmaceutical formulations. Also, the recoveries for cephadrine in spiked samples were found to be between 97% and 105%. We noted that the recoveries of the injection samples were in more than 100%. It may be resulted from some unknown interference species in the injection sample. Also, it is acceptable that the recovery falls in the range of 95–105%.

4. Conclusions

In summary, FSN-capped GNPs could respond selectively toward cephadrine degradation products, but not toward cephadrine and some excipients in pharmaceutical formulations, such as lactose, starch, gulemine, gelatine, sorbitol, glucose, fructose and sucrose maltose. The kinetics of cephadrine degradation products-induced GNPs aggregation could be significantly promoted by the increase of the ionic strength and temperature of the solution. The proposed method was successfully used for the sensitive and selective determination of cephadrine in pharmaceutical formulations, which can greatly develop the application of FSN-capped GNPs as sensors in pharmaceutical analysis.

Acknowledgements

This work was supported by the National Natural Science Foundation of China (Nos. 20975010, and 20907060). We are grateful to Professor Jin-Ming Lin for his support and encouragement.

References

- [1] J. Zhong, Z.G. Shen, Y. Yang, J.F. Chen, *Int. J. Pharm.* 301 (2005) 286.
- [2] G.J. Kemperman, R. Gelder, F.J. Dommerholt, P.C. Raemakers-Franken, A.J.H. Klunder, B. Zwanenburg, *Eur. J. Org. Chem.* (2001) 3641.
- [3] V.M. Johnson, J.P. Allanson, R.C. Causon, *J. Chromatogr. B* 740 (2000) 71.
- [4] P. Emaldi, S. Fapanni, A. Baldini, *J. Chromatogr. B* 711 (1995) 339.
- [5] A. Hilali, J.C. Jimenez, M. Callejon, M.A. Bello, A. Guiraum, *Talanta* 59 (2003) 137.
- [6] M. Hefnawy, Y. El-Shabrawy, F. Belal, *J. Pharm. Biomed. Anal.* 21 (1999) 703.
- [7] J. Yang, G. Zhou, X. Cao, Q. Ma, J. Dong, *Anal. Lett.* 31 (1999) 1047.
- [8] M. Kai, H. Kinoshita, K. Ohta, S. Hara, M.K. Lee, J.Z. Lu, *J. Pharm. Biomed. Anal.* 30 (2003) 1765.
- [9] Y.H. Li, J.R. Lu, *Luminescence* 21 (2006) 251.
- [10] R. Elghanian, J.J. Storhoff, R.C. Mucic, R.L. Letsinger, C.A. Mirkin, *Science* 277 (1997) 1078.
- [11] J.J. Storhoff, A.A. Lazarides, R.C. Mucic, C.A. Mirkin, R.L. Letsinger, G.C. Schatz, *J. Am. Chem. Soc.* 122 (2000) 4640.
- [12] K. Sato, K. Hosokawa, M. Maeda, *J. Am. Chem. Soc.* 125 (2003) 8102.
- [13] J.M. Nam, S.J. Park, C.A. Mirkin, *J. Am. Chem. Soc.* 124 (2002) 3820.
- [14] S. Mann, W. Shenton, M. Li, S. Connolly, D. Fitzmaurice, *Adv. Mater.* 12 (2000) 147.
- [15] J.J. Storhoff, R. Elghanian, R.C. Mucic, C.A. Mirkin, R.L. Letsinger, *J. Am. Chem. Soc.* 120 (1998) 1959.
- [16] J.W. Liu, Y. Lu, *J. Am. Chem. Soc.* 125 (2003) 6642.
- [17] S.Y. Lin, S.W. Liu, C.M. Lin, C.H. Chen, *Anal. Chem.* 74 (2002) 330.
- [18] S.Y. Lin, C.H. Chen, M.C. Lin, H.F. Hsu, *Anal. Chem.* 77 (2005) 4821.
- [19] Y.J. Kim, R.C. Johnson, J.T. Hupp, *Nano Lett.* 1 (2001) 165.
- [20] P.K. Sudeep, S.T.S. Joseph, K.G. Thomas, *J. Am. Chem. Soc.* 127 (2005) 6516.
- [21] S.J. Chen, H.T. Chang, *Anal. Chem.* 76 (2004) 3727.
- [22] F.X. Zhang, L. Han, L.B. Israel, J.G. Daras, M.M. Maye, N.K. Ly, C.J. Zhong, *Analyst* 127 (2002) 462.
- [23] C. Lu, Y.B. Zu, V.W.W. Yam, *Anal. Chem.* 79 (2007) 666.
- [24] C. Lu, Y.B. Zu, *Chem. Commun.* (2007) 3871.
- [25] M.A. Omar, O.H. Abdelmageed, T.Z. Attia, *Talanta* 77 (2009) 1394.
- [26] Z.Y. Zhong, S. Patskovskyy, P. Bouvrette, J.H.T. Luong, A. Gedanken, *J. Phys. Chem. B* 108 (2004) 4046.